*Geophys. J. Int.* (2003) **154,** 58–71

# Low-temperature magnetization and AC susceptibility of magnetite: effect of thermomagnetic history

Andrei Kosterov

*Earth and Planetary Science Department, Tokyo Institute of Technology,* 2-12-1 *Ookayama, Meguro, Tokyo* 152-8551, *Japan.*
*E-mail: kosterov@geo.titech.ac.jp*

Accepted 2003 January 20. Received 2003 January 16; in original form 2002 May 28

## SUMMARY

Saturation isothermal remanent magnetization (SIRM) and AC susceptibility have been measured as a function of temperature between 5 K and room temperature for one multidomain and three pseudo-single-domain magnetite samples after cooling in a zero (ZFC) and in a strong magnetic field (FC), and also after three partial field coolings (PFC) when a magnetic field had been turned on in 300–150, 150–80 and 80–5 K ranges, respectively. For the multidomain sample, SIRM(5 K) after ZFC is about twice as high as after FC, while the low-field susceptibility is higher after FC. SIRM and susceptibility curves measured after PFC(300–150 K) and PFC(150–80 K) coincide with those measured, respectively, after ZFC and FC. PFC(80–5 K) curves are intermediate between the two extremes. This behaviour can be fairly well understood within the framework of a simple model, introduced back in the 1950s, which assumes that on cooling through the Verwey transition in a strong magnetic field easy magnetization axes in the low-temperature phase are set along the [001] directions of the high-temperature (cubic) phase closest to the field direction. If, on the other hand, the Verwey transition is passed in a zero field and a strong magnetic field is applied below the transition temperature, some of easy axes, initially set at random, can still be switched into the field direction, explaining observed SIRM and susceptibility versus temperature curves measured after PFC(80–5 K). Pseudo-single-domain grains show a more complex behaviour, which depends strongly on sample stoichiometry. In two samples with a relatively small non-stoichiometry (Verwey temperatures are 122 and 110 K, respectively) SIRM(5 K) is higher by 5–7 per cent after FC. After both PFC(150–80 K) and PFC(80–5 K), SIRMs are nearly equal in magnitude to SIRM acquired after FC, but are thermally demagnetized at a different rate below the Verwey transition. Low-field susceptibilities also show different temperature dependences below $T_V$, dependent on a preceding thermomagnetic treatment. A strongly non-stoichiometric sample ($T_V = 95$ K) shows very large, over 70 per cent, difference between SIRMs after FC and ZFC, respectively, and a 35 per cent difference between susceptibilities measured under the same conditions. These results suggest that in magnetite grains several microns in size, easy magnetization axes setting on first passing the Verwey transition from above and switching of easy axes on subsequent cooling below the transition occur, qualitatively, in the same way as in grains of larger size, but switching of easy axes is considerably facilitated. The latter process is subject to further enhancement in strongly non-stoichiometric magnetite, where it seems to be possible even in zero field, resulting in SIRM, susceptibility and magnetic hysteresis properties fairly different from more stoichiometric samples. Strongly depressed, compared with stoichiometric magnetite, magnetocrystalline anisotropy of the low-temperature phase could be a physical mechanism for this behaviour.

**Key words:** magnetic domains, magnetite, Verwey transition.

## 1 INTRODUCTION

Low-temperature magnetic properties of mineral magnetite and magnetite-bearing rocks have come under scrutiny in palaeo- and rock magnetism since it was realized, in the early 1960s, that a magnetization anomaly (Weiss & Forrer 1929) on passing the Verwey phase transition (Verwey 1939) offers a convenient method for detecting magnetite in rocks (Nagata *et al.* 1964), while

cycling magnetite-bearing rocks to 77 K in zero field (low-temperature cleaning) could remove unwanted secondary magnetizations carried by magnetite (Ozima *et al.* 1964b). Apart from mineral magnetite, the initial research was largely conducted on volcanic rocks (Nagata *et al.* 1964; Ozima & Ozima 1965; Creer & Like 1967); however, Mauritsch & Turner (1975) have pioneered use of low-temperature magnetometry in studies of magnetic mineralogy of sedimentary rocks. Initial susceptibility measurements between 77 K and room temperature (RT) have also been used for the characterization of magnetic mineralogy of basalts (Radhakrishnamurty *et al.* 1981; Senanayake & McElhinny 1981, 1982). More recently, with the advent of commercial systems capable of measuring magnetization and/or susceptibility down to and below 4.2 K, low-temperature magnetometry of minerals and rocks, and most notably of magnetite, has seen a new boost. Apart from the simplest task of magnetite detection in a rock, the research scope has broadened to include the magnetic hysteresis properties (Schmidbauer & Schembera 1987; Schmidbauer & Keller 1996; Kosterov 2001, 2002; Özdemir *et al.* 2002; Smirnov & Tarduno 2002) and magnetic domain structure (Moloni *et al.* 1996) of the low-temperature phase itself, and also, in pace with the developments in solid-state physics (Walz 2002), studies into the effect of oxidation (Özdemir *et al.* 1993; Cui *et al.* 1994) and stress (Sahu 1997; King & Williams 2000) on the Verwey transition temperature and magnetization variation across the transition.

In the physics of magnetic materials, it has long been known that magnetic properties of the low-temperature phase of magnetite are largely controlled by the magnetic field applied during cooling through the Verwey transition (Li 1932; Bickford 1950; Domenicali 1950). A model that accounts for most of the observed features (Bickford 1950; Williams *et al.* 1953) assumes that cooling in a strong magnetic field sets an easy magnetization axis of the low-temperature phase approximately along the [001] direction of the high-temperature (cubic) phase closest to the field direction. Alongside with this process, switching of easy axes into a new direction below the Verwey transition, made possible by applying a strong magnetic field at a large angle to an initial easy axis, has been observed (Bickford 1950; Calhoun 1954; Abe *et al.* 1976). This model is qualitatively consistent with the observed magnetic hysteresis properties of the low-temperature phase of multidomain magnetite with the grain size 100–150 μm (Kosterov 2001), where the $M_{rs}/M_s$ ratio and the coercive force were both much lower after field cooling (FC) compared with the values after zero-field cooling (ZFC). In contrast, in pseudo-single-domain magnetite (grain size <5 μm) a considerably more complex behaviour has been observed, which includes a number of peculiar features: (1) a rapid decrease with increasing temperature of the $M_{rs}/M_s$ ratio after FC; (2) an equally rapid decrease with increasing temperature of the coercive force after ZFC; (3) a small but discernible difference between the $H_c(T)$ curves measured after the two different ZFC treatments, one being started, at room temperature, from a magnetized, and another from a demagnetized state (Kosterov 2001, 2002); (4) a non-monotonic dependence of the $M_{rs}/M_s$ ratio in the low-temperature phase on the magnitude of the magnetic field applied during cooling; (5) an induced magnetic anisotropy at temperatures below the Verwey transition after cooling in magnetic fields between 10 and 90 mT; and (6) a non-monotonic dependence of a low-temperature (10 K) remanent magnetization resulting from cooling through the Verwey transition in a non-zero magnetic field on the field intensity (Smirnov & Tarduno 2002). All of these features have been observed in both stoichiometric and non-stoichiometric samples. Since measurement of the complete hysteresis loops as a function of temperature is generally a very time-consuming experiment, it appeared to be of interest to study the temperature dependences of magnetization and susceptibility below the Verwey transition and compare them with already known hysteresis properties at these temperatures.

## 2 SAMPLES

In the present study, four magnetite samples for which magnetic hysteresis properties below the Verwey transition had been studied previously (Kosterov 2001, 2002) were used. Two of them were sieved fractions (<5 and 100–150 μm) of the crushed natural magnetite sample HM4 (Hartstra 1982), designated as HM4S and HM4L, respectively. Another two samples were commercially produced magnetites, designated as BK-5099 (Pfizer Company) and 3006 (Wright Company). Sample 3006 with the nominal grain size 2–3 μm had been acquired in 1999 (A. Smirnov, personal communication, 1999) and sample BK5099 in 1981 (Ö. Özdemir, personal communication, 1999). For BK5099, room-temperature magnetic properties and grain size distribution had been measured by Özdemir & Banerjee (1982). Using TEM, they found the mean grain size to be 0.12 μm, and minimum and maximum sizes of 0.05 and 0.6 μm, respectively. Grains were mostly of spherical or cubic shape. In sample 3006, grains are of a rather irregular shape and have a fairly broad size distribution, from 0.5 μm to about 5 μm. HM4S appears to contain a more or less uniform distribution of grains in the 1–5 μm range, and significantly less abundant 0.5–0.7 μm grains. HM4L contains a roughly uniform distribution of 100–150 μm grains, and very little, if any, significantly smaller ones. In both size fractions of HM4 grains are equant or slightly elongated and reveal evident traces of crushing.

According to the microprobe analysis (Hartstra 1982), major impurities in the HM4 sample are magnesium (4.8 per cent), aluminium (0.9 per cent) and manganese (0.6 per cent). No major impurities have been reported for 3006 and BK5099 magnetites. High-temperature susceptibility curves for the four samples were measured with a KLY-3 instrument in argon atmosphere. All samples yielded a single Curie point in the 585–590 °C range, i.e. just slightly higher than the nominal value for the stoichiometric magnetite. Room-temperature hysteresis loops of the four samples were measured with a Princeton Measurements vibrating sample magnetometer in a maximal field 1.4 T prior to the low-temperature experiments (Kosterov 2001, 2002) and the respective hysteresis parameters are listed in Table 1. For HM4L, room-temperature hysteresis parameters are in the multidomain range, consistent with its grain size. For the three finer samples, they all lie in the pseudo-single-domain range; however, the $M_{rs}/M_s$ and $H_{cr}/H_c$ ratios for HM4S and 3006 are somewhat high compared with the general trend for crushed magnetite grains (Dunlop 1995, 2002), and for BK5099 they are somewhat low. In the two former samples, this discrepancy is probably due to relatively high stresses to which these samples have been subject during crushing or manufacture process. BK5099, which has the smallest grain size of all the samples used in the present study, is severely oxidized because of air exposure for 20 yr and its superficial layer is probably totally converted to maghemite (Kosterov 2002). This may account for the lowering of the $M_{rs}/M_s$ ratio and coercivity compared with the stoichiometric magnetite.

**Table 1.** Room-temperature magnetic hysteresis parameters and apparent Verwey temperatures for the four samples used in the present study. Low-temperature hysteresis properties of these samples have been reported previously (Kosterov 2001, 2002).

| Sample | $M_{rs}/M_s$ | $H_c$ (mT) | $H_{cr}$ (mT) | $H_{cr}/H_c$ | Mean Verwey temperature (K) | | |
|---|---|---|---|---|---|---|---|
| | | | | | From low-$T$ hysteresis | From SIRM | From $\chi'$ |
| HM4L | 0.025 | 2.06 | 9.02 | 4.38 | 115 | 117.5 | 117.5 |
| HM4S | 0.30 | 29.5 | 41.9 | 1.42 | 119 | 122 | 122 |
| 3006 | 0.30 | 24.5 | 38.7 | 1.58 | 108 | 112 | 107 |
| BK5099 | 0.17 | 11.3 | 24.7 | 2.19 | n.d. | 95 | 90 |

## 3 EXPERIMENT

Two quantities, saturation isothermal remanent magnetization (SIRM) and AC complex susceptibility, $\chi = \chi' - i\chi''$, have been measured as a function of temperature between 5 and 300 K. Since below the Verwey transition both parameters are thought to be controlled by the distribution of easy magnetization axes in the low-temperature phase (Li 1932; Bickford 1950; Williams *et al.* 1953), SIRM and susceptibility warming curves have been measured five times: after a zero-field cooling, after a field cooling and after three different partial field coolings (PFCs) (Smirnov & Tarduno 2000), when the magnetic field was turned on only in a certain temperature range. Thereafter, for the sake of brevity, an SIRM or a $\chi$ curve measured after any of these treatments will be designated by an abbreviation of the respective treatment. Temperature intervals for partial field coolings were, respectively, 300–150, 150–80 and 80–5 K. A 5 T magnetic field was used for FCs and PFCs. After an initial cooling, an SIRM was imparted with a 5 T field, then the magnetic field was switched off, and measurement of either SIRM or susceptibility started after a 60 s pause. To measure an AC susceptibility, an alternating field of 100 μT peak amplitude at 10 Hz frequency was generally used. Besides these measurements, taken on warming only, SIRM evolution (after initial ZFC) was monitored during two consecutive 6–300–6 K cycles in zero field. Also, temperature evolution of an SIRM given at 300 K was measured in zero field during two consecutive 300–6–300 K cycles. Finally, the frequency dependence of susceptibility was measured in the frequency range $10^{-2}$–$10^{3}$ Hz at room temperature and at a few selected temperatures below the Verwey transition. All magnetic measurements at low temperatures were carried out using an MPMS XL instrument at the Geological Survey of Japan.

## 4 REMANENCE BEHAVIOUR

### 4.1 Zero-field warming

SIRM warming curves are summarized in Fig. 1. The multidomain sample HM4L exhibits a relatively simple behaviour, much like that reported previously (Aragón 1992; Özdemir & Dunlop 1999): little variation below and above the Verwey transition, and a sharp drop of magnetization in a narrow temperature interval associated with the transition. In HM4L, the drop occurs between 116 and 119 K, yielding an apparent transition temperature of 117.5 K. It is, however, worth noting that in the magnetic hysteresis experiments on the same sample (Kosterov 2001) an increase of $M_s$ and a drop of $M_{rs}$ and of the coercive force have been observed at a slightly lower temperature, between 114 and 116 K. The mode of cooling through the transition strongly affects the sample. SIRM after ZFC is almost twice as high as after FC. Nearly the same relationship has been found previously for this sample (Kosterov 2001) between $M_{rs}/M_s$ ratios derived from hysteresis loops measured at low temperature after the two treatments. These observations can be qualitatively explained in terms of the simple model developed by Bickford (1950) and Williams *et al.* (1953). According to it, below the Verwey transition easy magnetization axes are distributed at random after ZFC, while after FC they are concentrated within the cone with the conical angle 54.73° around the field direction. Critical fields (microcoercivities) due to domain walls displacement are expected to vary as $H_{c0}/\cos\theta$, where $\theta$ is the angle between magnetization within the domains and the external field and $H_{c0}$ is a critical field for $\theta = 0$. The bulk coercive force would then be higher for a grain assemblage in which relatively larger fraction of grains have easy magnetization axes directed at large angles with respect to the external field. Since in multidomain grains saturation remanence is related to coercivity through the demagnetizing factor, SIRM would also be larger after ZFC. Applicability of this model is corroborated by the PFC(300–150 K) and PFC(150–80 K) SIRM warming curves. The latter practically coincides with the FC curve, and the former with the ZFC curve, showing that no permanent axis switching occurs above $T_V$, and, on the other hand, the process of easy axes setting is complete by 80 K. However, if the magnetic field is *first* applied well below $T_V$, switching of some easy axes into new directions is still possible as shown by the PFC(80–5 K) curve.

SIRM curves of three other samples (Figs 1b–d ) differ significantly from those of HM4L. Magnetization decrease due to the Verwey transition is much smaller than for HM4L, and occurs in a rather wide, 20–30 K, temperature range. Apparent transition temperatures, deduced from the SIRM derivative curves are, respectively, 122 K for HM4S, 112 K for 3006 and 95 K for BK5099, probably reflecting the difference in the stoichiometry of the samples. In the two former samples, most of the volume seems to remain relatively stoichiometric, and the behaviour of their SIRM curves has much in common. SIRM after FC is slightly higher than after ZFC, as are SIRMs after PFC(150–80 K) and PFC(80–5 K). However, the two latter curves show a significant difference below the Verwey transition, SIRM after PFC(150–80 K) being much more stable. This observation is consistent with a hypothesis that easy axes established on passing the Verwey transition are more stable than those switched into below the transition. On the other hand, close similarity of PFC(80–5 K) and FC curves shows that easy axes established on passing the transition are vulnerable to further switching when placed in a strong field. Showing many common features in the behaviour below and at the Verwey transition, SIRMs of the two samples decay at different rates above it. This can be viewed as evidence for the presence of a superficial maghemite layer in 3006 and its absence in HM4S. Indeed, SIRM of pure maghemite decreases quite significantly between 77 K and room temperature (Morrish & Watt 1958; de Boer & Dekkers 1996), and the presence of maghemite in magnetite sample

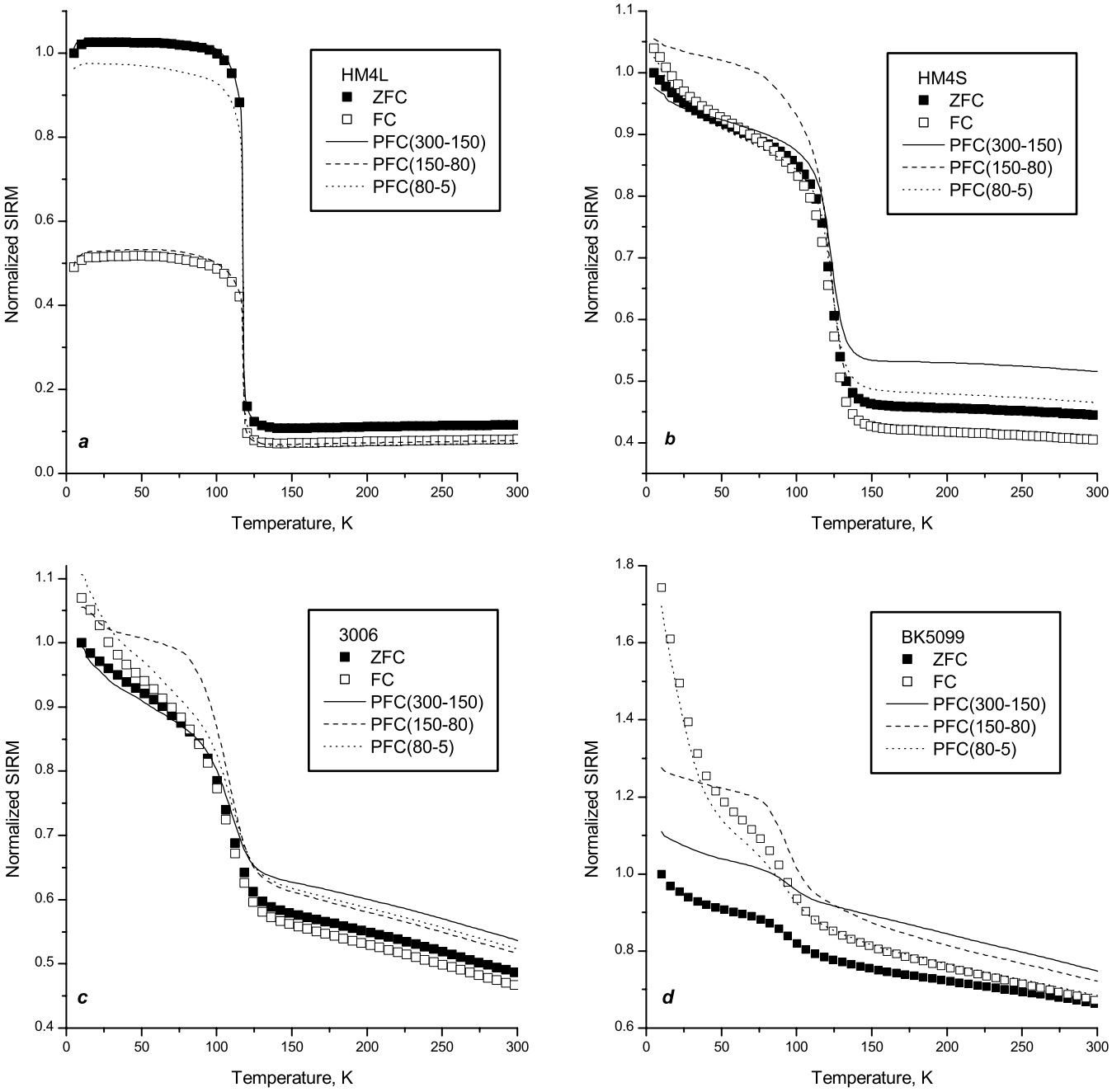


**Figure 1.** Low-temperature demagnetization curves of SIRMs acquired at 5 K after different thermomagnetic treatments.

3006 has been directly demonstrated by reducing it to apparently stoichiometric composition by heating in a $CO/CO_2$ atmosphere (Smirnov & Tarduno 2002).

BK5099, which has the smallest grain size of the four studied samples, shows a completely different behaviour. SIRM after FC is much larger then after ZFC, and the inspection of SIRMs measured after different PFCs (Fig. 1d) shows that this difference is mostly produced below 80 K. The PFC(80–5 K) curve almost replicates the FC one. At the same time, SIRM after PFC(150–80 K) is much more stable against warming below 80 K, but, on the other hand, a relatively larger fraction of the latter is lost at the Verwey transition. This behaviour is thought to be generally related to a greater degree of non-stoichiometry of the sample, reflected by its lower $T_V$ (95 K). Indeed, it has been demonstrated experimentally (Kąkol & Honig 1989) that easy axis switching is greatly facilitated in strongly non-stoichiometric magnetites. Easy axis switching is also probably the origin of the anomalous hysteresis properties of this sample at low temperatures (Kosterov 2002).

### 4.2 Zero-field cycling

The results of zero-field cycling of the room-temperature SIRM are summarized in Fig. 2. PSD samples show the behaviour generally comparable with their grain size and rather highly stressed state. The fraction of SIRM remaining after the first low-$T$ cycle (second memory as defined by Özdemir *et al.* 2002) is, respectively, 64 per cent for HM4S, 73 per cent for 3006 and

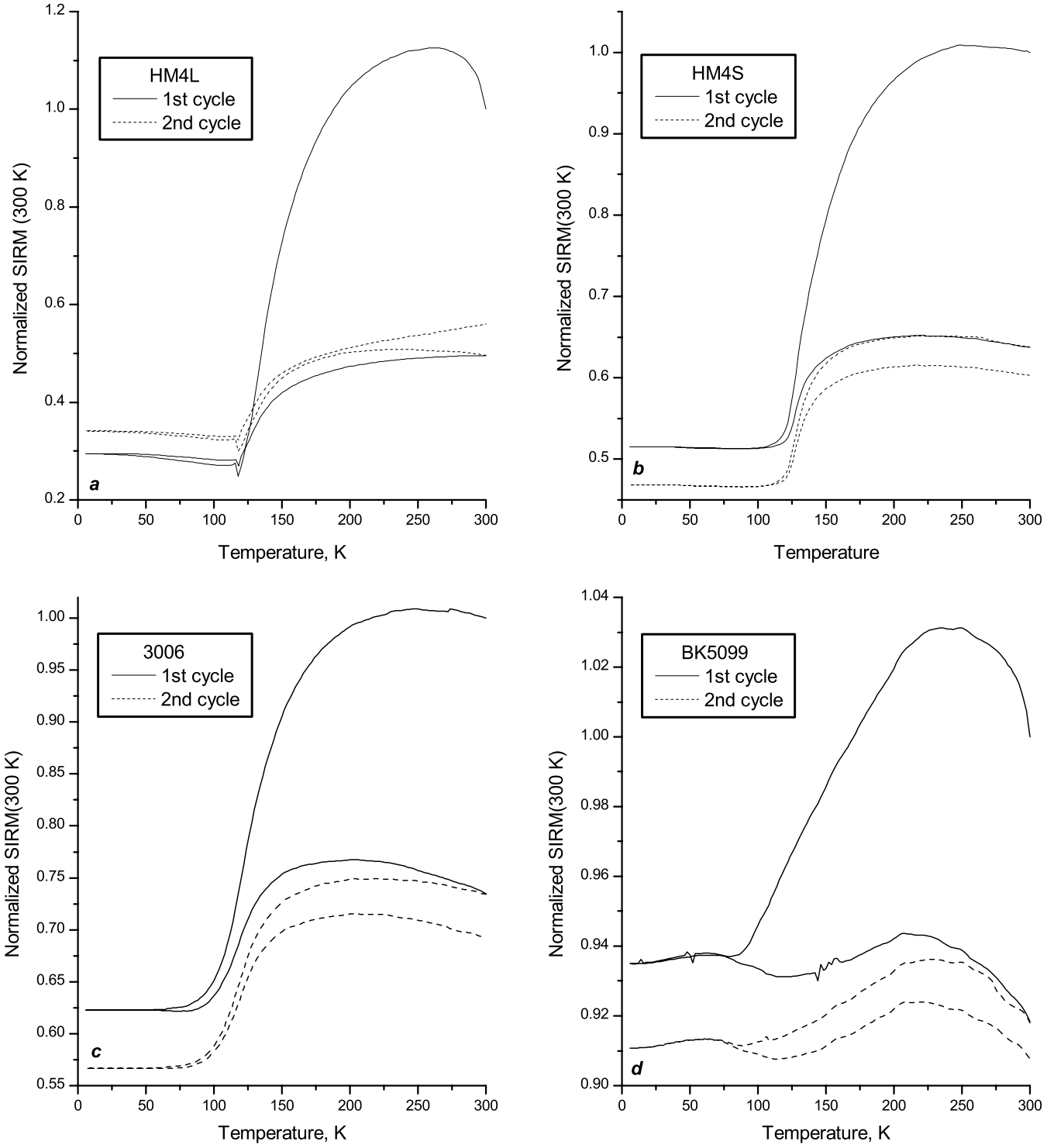


**Figure 2.** The behaviour of SIRM acquired at 300 K during two consecutive cycles to 6 K in zero field.

92 per cent for BK5099. The high SIRM memory of BK5099 is probably due to a combined effect of its fine grain size and the presence of a substantial amount of maghemite, which does not show loss of remanence in the low-temperature cycling (de Boer & Dekkers 1996). A second low-temperature cycle results in a further, by a few per cent, decrease of magnetization recovered at room temperature, similar to that reported previously (Kobayashi & Fuller 1968). At the same time, it is worth noting that the respective warming curves for the first and the second cycle are very similar in shape (Fig. 2). The MD sample HM4L also shows some recovery of remanence on passing the Verwey transition from below, and SIRM memory is about 40 per cent (Fig. 2a), which is evidence for a highly stressed state (Heider *et al.* 1992; King & Williams 2000). At the Verwey transition, a rebound of magnetization is observed, similar to that found previously in large MD grains (Halgedahl & Jarrard 1995; Özdemir & Dunlop 1998,

1999; Muxworthy & McClelland 2000; Özdemir *et al.* 2002). It is interesting to note that in the second cycle, the magnetization (SIRM memory) decreases more slowly than it increased during warming in the first cycle. Slightly higher magnetization is then produced at 6 K, and at room temperature after the termination of the second cycle.

Temperature cycles of SIRM imparted at 6 K (Fig. 3) are qualitatively different from those of the room-temperature SIRM, in accord with previous observations (Ozima *et al.* 1964a; Kobayashi & Fuller 1968; Özdemir *et al.* 2002). As described above (Section 4.1) the first warming through the Verwey transition results in a major loss of remanence, while the behaviour during the cooling part of the first cycle and during the entire second cycle is quite different for MD and PSD grains. In PSD samples, magnetization shows only a small variation during cooling of the room-temperature residue of the low-temperature SIRM, and during the subsequent warming–cooling

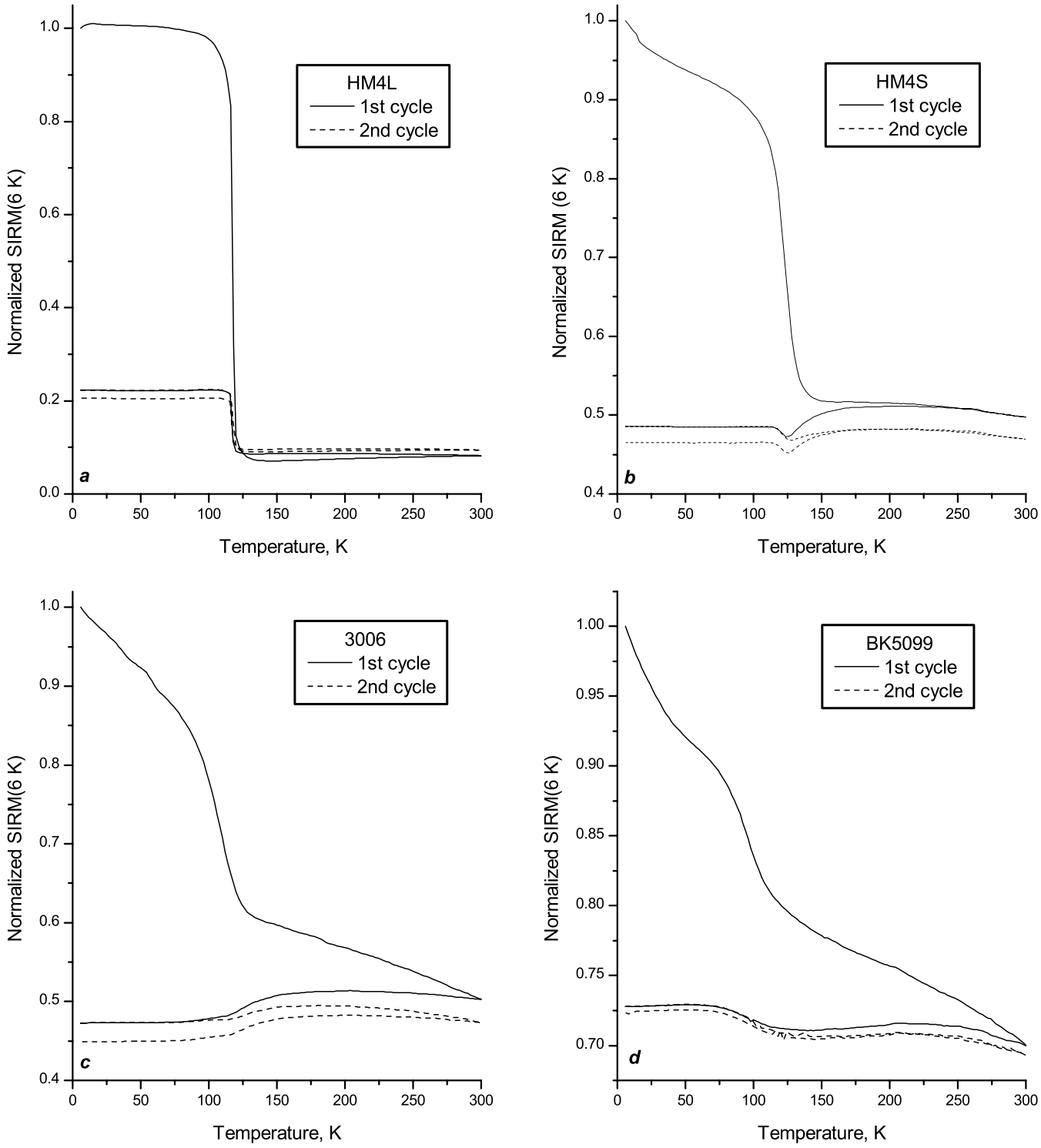


**Figure 3.** The behaviour of SIRM acquired at 6 K during two consecutive cycles to 300 K in zero field.

cycle. However, details vary somewhat from sample to sample. For HM4S (Fig. 3b), the room-temperature residue first slightly increase on subsequent cooling, almost following the precedent warming curve down to about 240 K, and then starts to decrease approaching the Verwey transition. At the transition, a small rebound of magnetization is observed, which is then reversed during rewarming. A similar magnetization rebound is also observed on the second cooling. In samples 3006 and BK5099, on the other hand, a relatively strong decrease of magnetization above the Verwey transition during first warming is not replicated during cooling. This suggests that decreasing magnetization above $T_V$ in these two samples is due to the presence of a significant amount of maghemite, apparently absent in HM4S. Upon cooling, magnetization of 3006 decreases monotonically, and shows an increase, albeit very small, on passing the Verwey transition during the second warming. In BK5099, magnetization increases slightly on passing the transition from above, and decreases by about the same amount when passing the $T_V$ from below in the second cycle. MD sample HM4L shows a qualitatively different behaviour similar to that observed previously by Kobayashi & Fuller (1968): the room-temperature residue shows a fairly strong rebound during the first cooling, followed in the second cycle by an almost reversible variation with magnetization loss and rebound at $T_V$.

Since SIRMs acquired in both high- and low-temperature phases have been monitored during two consecutive zero-field cycles, it is possible to directly compare RT–6 K–RT cycles for the two starting magnetic states: the residue of the low-temperature SIRM after warming through $T_V$ to the room temperature (designated in the following as $\mathrm{SIRM}_{\mathrm{lt}}^{(\mathrm{I})}$), on one hand, and the residue of the room-temperature SIRM after the complete RT–6 K–RT cycle (second memory following the terminology of Özdemir *et al.* 2002, designated here as $\mathrm{SIRM}_{\mathrm{rt}}^{(\mathrm{II})}$). These curves are shown in Fig. 4, normalized in each case to a starting remanence value at room temperature. Several features are noteworthy. In both cases, remanence first increases slightly, roughly in proportion to $M_s$. Below about 250 K, two cooling curves start to diverge, demagnetization being much more intense for $\mathrm{SIRM}_{\mathrm{rt}}^{(\mathrm{II})}$. $\mathrm{SIRM}_{\mathrm{lt}}^{(\mathrm{I})}$, on the other hand, demagnetizes only slightly for the three pseudo-single-domain samples, while for the multidomain sample HM4L the magnetization at a local minimum at 132 K is even higher than the starting room-temperature value. Signature of the Verwey transition in the cooling curves of the two states is also fairly different. In the case of $\mathrm{SIRM}_{\mathrm{rt}}^{(\mathrm{II})}$, in three pseudo-single-domain samples remanence continues to demagnetize to a temperature about 10–15 K below the Verwey transition. Only in the multidomain sample HM4L does remanence show a small rebound at the transition similar to that observed on this sample in the first cooling of room-temperature SIRM. In contrast, for the $\mathrm{SIRM}_{\mathrm{lt}}^{(\mathrm{I})}$ a small but distinctive rebound of magnetization associated with the transition is seen in two out of three studied pseudo-single-domain samples, and in the third one, sample 3006, a break-in-slope is seen slightly above the transition temperature assumed to be 110 K. Sample HM4L shows in this case a very strong remanence rebound, magnetization below the transition increasing by a factor of 2.7. In the low-temperature phase itself, magnetization changes reversibly in all cases, in accord with previous observations (Özdemir & Dunlop 1999; Muxworthy & McClelland 2000; Özdemir *et al.* 2002). On the subsequent warming, once the Verwey transition is passed, magnetization variation nearly mirrors that during cooling, i.e. stronger remanence loss (in the case of $\mathrm{SIRM}_{\mathrm{rt}}^{(\mathrm{II})}$) is matched by a stronger rebound and vice versa. As a result, second memories of $\mathrm{SIRM}_{\mathrm{rt}}^{(\mathrm{II})}$ and $\mathrm{SIRM}_{\mathrm{lt}}^{(\mathrm{I})}$ nearly equal each other.

## 5 LOW-FIELD SUSCEPTIBILITY

### 5.1 Temperature dependences

Variation of the in-phase initial susceptibility $\chi'$ with temperature is shown in Fig. 5. HM4L shows a step-like increase of susceptibility at the $T_V$, similar to that observed previously on the grains of similar or larger size (Moskowitz *et al.* 1998; Muxworthy 1999; Skumryev *et al.* 1999). Cooling through the transition in the strong magnetic field results in higher susceptibility than that in zero field, directly reflecting the concentration of easy magnetic axes around the direction of the field applied during FC. Susceptibility after PFC(80–5 K) almost equals that after FC and PFC(150–80 K), indicating that easy axes distributions at 5 K forming after the three treatments are similar. On the other hand, on the consequent warming the PFC(80–5 K) curve tends towards the ZFC one, implying a different thermal stability of the easy axes switched into by a strong magnetic field applied below 80 K.

In pseudo-single-domain samples HM4S and 3006 susceptibility increase associated with the Verwey transition is much more gradual (Figs 5b and c), also in agreement with previous observations (Muxworthy 1999). Field cooling results in higher susceptibility values at 5 K, and in a smaller temperature variation on subsequent warming, so that ZFC and FC curves converge well below the respective Verwey temperatures, at approximately 100 K for HM4S and at 90 K for 3006. An interesting behaviour is observed after PFC(150–80 K) and PFC(80–5 K): for both samples these susceptibility curves differ from each other, and both of them also differ from the respective FC curves. In the PFC(150–80 K) curves even a break-in-slope, corresponding to the switching off of the field during cooling, can be seen near 80 K.

In general, two characteristic regimes can be recognized in the temperature dependences of the low-field susceptibility below the Verwey transition, independent of the mode of preceding cooling through $T_V$. Both ZFC and FC susceptibilities first slightly decrease with increasing temperature, reaching a minimum at 12–13 K, and then increase gradually with temperature until 35 K in sample HM4L and until 50 K in HM4S and 3006. Similar behaviour has been observed previously, being in addition frequency dependent (Muxworthy 1999; Skumryev *et al.* 1999). The frequency dependence of susceptibility at 10 and 30 K has been observed in the present study as well (see Section 5.2). At higher temperatures the susceptibility behaviour is fairly different for multidomain and pseudo-single-domain grains. In the former, both ZFC and FC susceptibilities decrease gently, again similar to previous studies (Moskowitz *et al.* 1998; Muxworthy 1999; Skumryev *et al.* 1999). In contrast, in pseudo-single-domain grains ZFC susceptibility continues to increase, albeit at a slower rate, while FC susceptibility flattens out. This is in accordance with the decrease of the coercive force with increasing temperature after ZFC and its constancy after FC (Kosterov 2001, 2002).

Sample BK5099, which contains smaller grains and is considerably stronger oxidized that two other pseudo-single-domain samples in the present study, shows a somewhat different behaviour (Fig. 5d). At 5 K, the in-phase susceptibility after FC is higher than that after FC by about 35 per cent. This difference is more than twice as large as in HM4S and 3006. The susceptibility curve measured after PFC(150–80 K) almost coincides with the ZFC one, and that measured after PFC(80–5 K) with the FC one. The two regimes in susceptibility versus temperatures curves described above can still be recognized, but they are significantly less distinct, with only a small break in slope around 50 K.

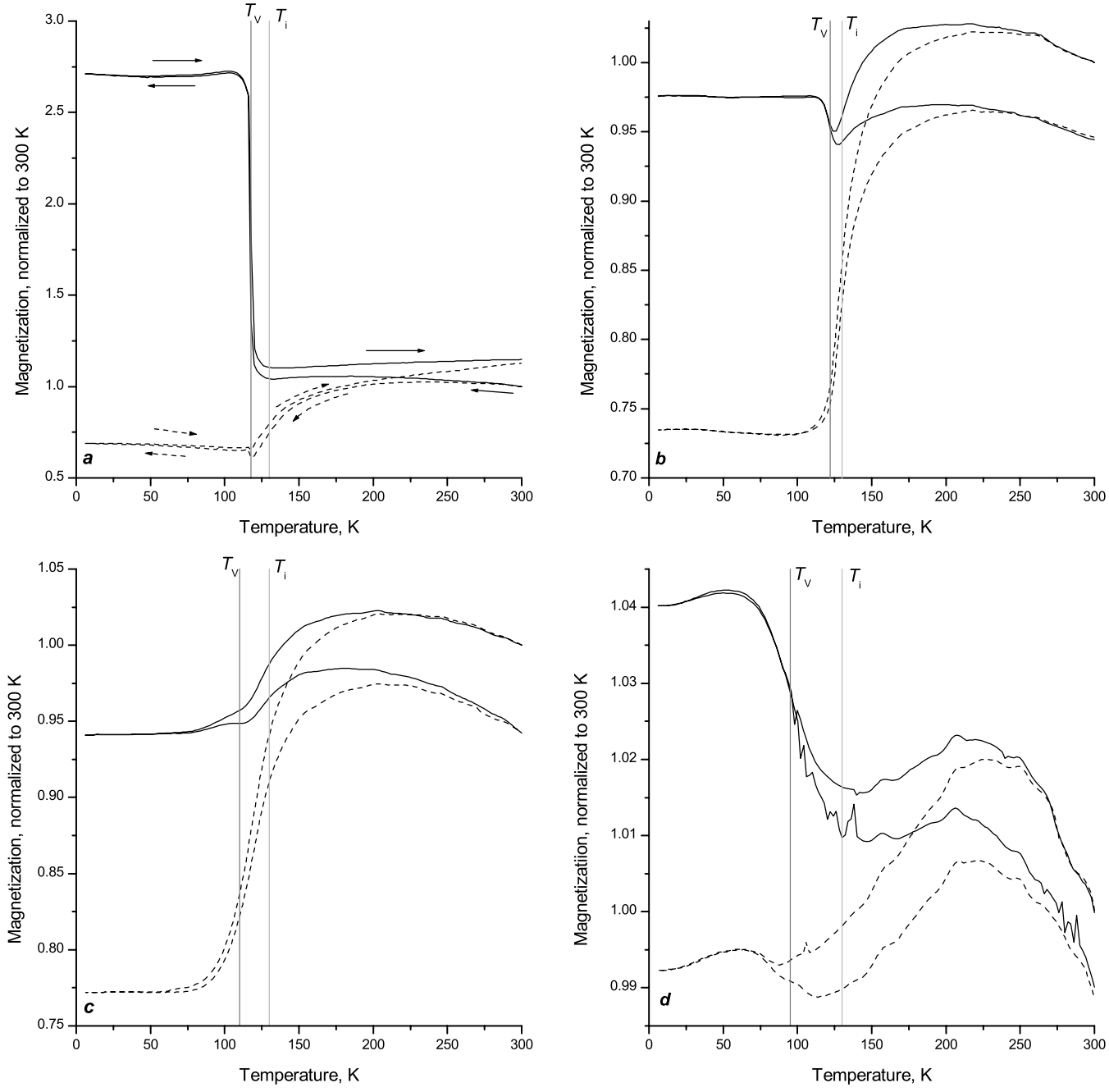


**Figure 4.** A comparison of 300–6–300 K zero-field cycles for a 300 K residue of an SIRM given at 6 K (solid lines) and a residue of an SIRM given at 300 K after a complete zero-field cycle to 6 K (dashed lines). (a) Sample HM4L; (b) sample HM4S; (c) sample 3006; (d) sample BK5099. Verwey transition temperatures ($T_V$) were determined from SIRM($T$) warming curves (Table 1), isotropic point ($T_i$) is taken to be 130 K in all cases.

Another parameter that can yield information concerning the magnetic state of a ferromagnetic sample is the out-of-phase susceptibility. When a sample is subjected to an AC magnetic field, the resulting induced magnetization usually has a small component orthogonal to the field, so that the total susceptibility can be written in the form $\chi = \chi' - i\chi''$, where $\chi'$ is the usual in-phase susceptibility, and $\chi''$ is the out-of-phase susceptibility. The temperature variation of the susceptibility phase angle $\varphi$, which is related to $\chi''$ through the equation $\varphi = \tan^{-1}(\chi''/\chi')$, for the four samples studied is shown in Fig. 6. Two features are observed in all cases: a peak in the 15–30 K range, and a peculiar double-jump (triple in the case of HM4L) at 122 and 144 K, respectively. The peak at about 30 K has been observed previously on large single crystals of stoichiometric magnetite (Šimša *et al.* 1985; Skumryev *et al.* 1999), and its origin is thought to be related to a certain type of relaxation of domain walls. However, in the present study the peak is observed on supposedly isotropic assemblages of magnetite grains, and three out of four samples have a grain size of about 5 μm at most. The magnitude of the low-temperature peak depends on the preceding magnetic treatment being significantly higher after FC. This agrees qualitatively with the domain walls relaxation as an origin for this effect, thereby indicating that below the Verwey temperature a

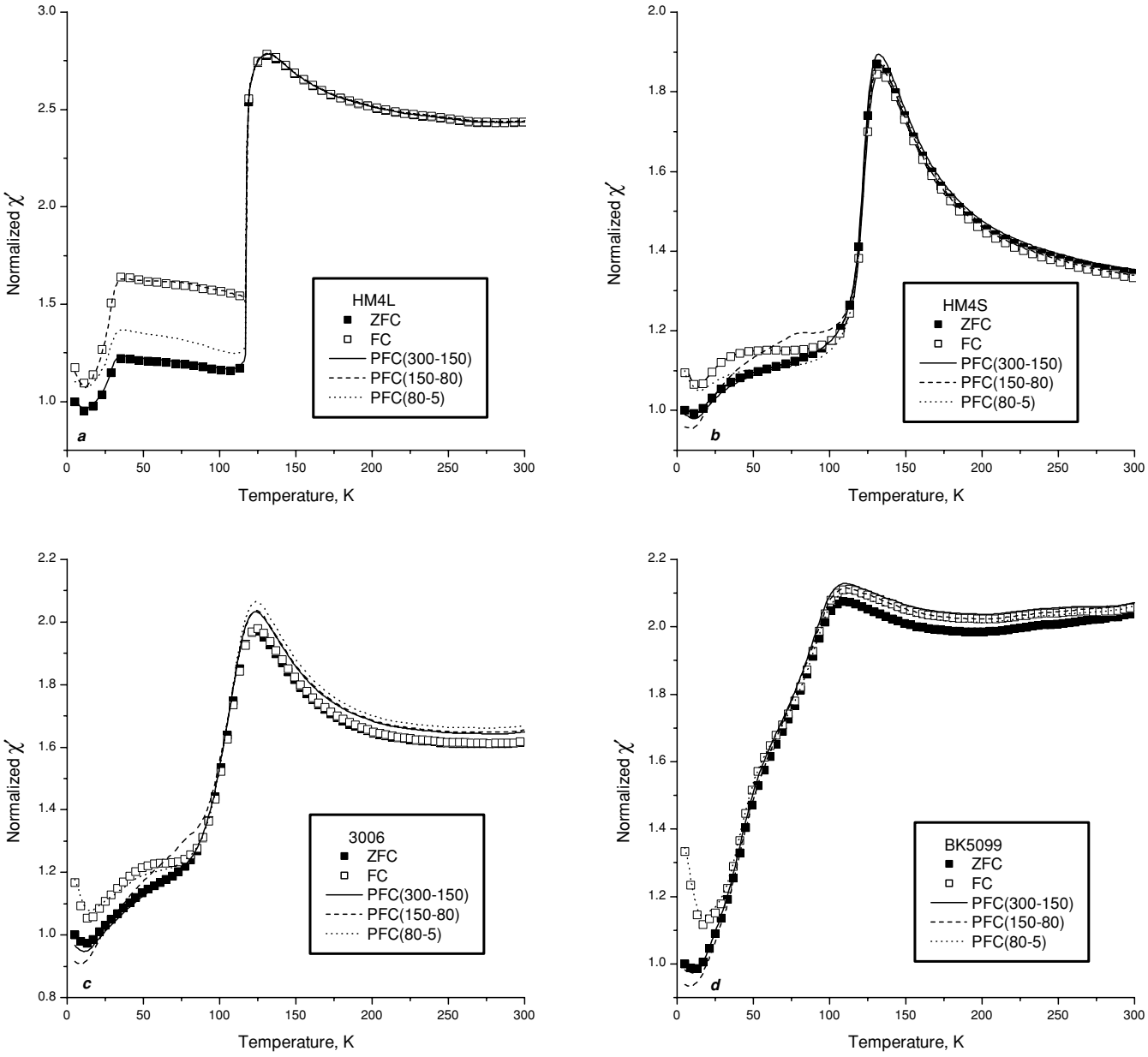


**Figure 5.** Temperature dependences of the in-phase susceptibility after different thermomagnetic treatments.

structure with distinct domain walls exists even in fairly small grains, in agreement with hysteresis data (Kosterov 2001, 2002). With decreasing grain size, the magnitude of the $\chi''$ peak (measured as the phase angle $\varphi$) decreases, and also shifts towards lower temperatures, from 28 K for HM4L to about 17–20 K for the three other samples. BK5099, however, shows a more complex behaviour with another, apparently treatment-independent peak at 35 K.

In the vicinity of the Verwey transition, all four samples show a similar $\chi''$ pattern with jumps at 122 and 144 K as the main features. The jump at 122 K seems to be a direct manifestation of the Verwey transition, since the difference between ZFC and FC curves largely disappears exactly at this temperature. The origin of the 144 K jump is not clear, but it has been observed beyond measurement errors in all four samples used in the present study. In view of apparently different Verwey temperatures, obtained from SIRM and in-phase susceptibility measurements, and also from the magnetic hysteresis data (Kosterov 2001, 2002), it seems amazing that such a persistent pattern is observed in $\chi''$ behaviour in the samples of apparently different stoichiometry. It may be suggested then that this double-jump pattern in $\chi''$ temperature dependence is a manifestation of truly stoichiometric magnetite. If this is indeed so, it means that even in the severely oxidized sample BK5099 a certain amount of stoichiometric magnetite still exists, probably in the very inner parts of the grains.

Being otherwise the closest to the model stoichiometric magnetite, HM4L shows a somewhat more complex behaviour in terms of $\chi''$. An additional jump is observed at 118 K, which is even larger than the following jump at 122 K. Note that the temperature of the first jump corresponds fairly well to the temperature range where the major drop of magnetization and the increase of the in-phase susceptibility occurs. Since the single-stage model of the Verwey transition now seems to be the only viable model, at least in the

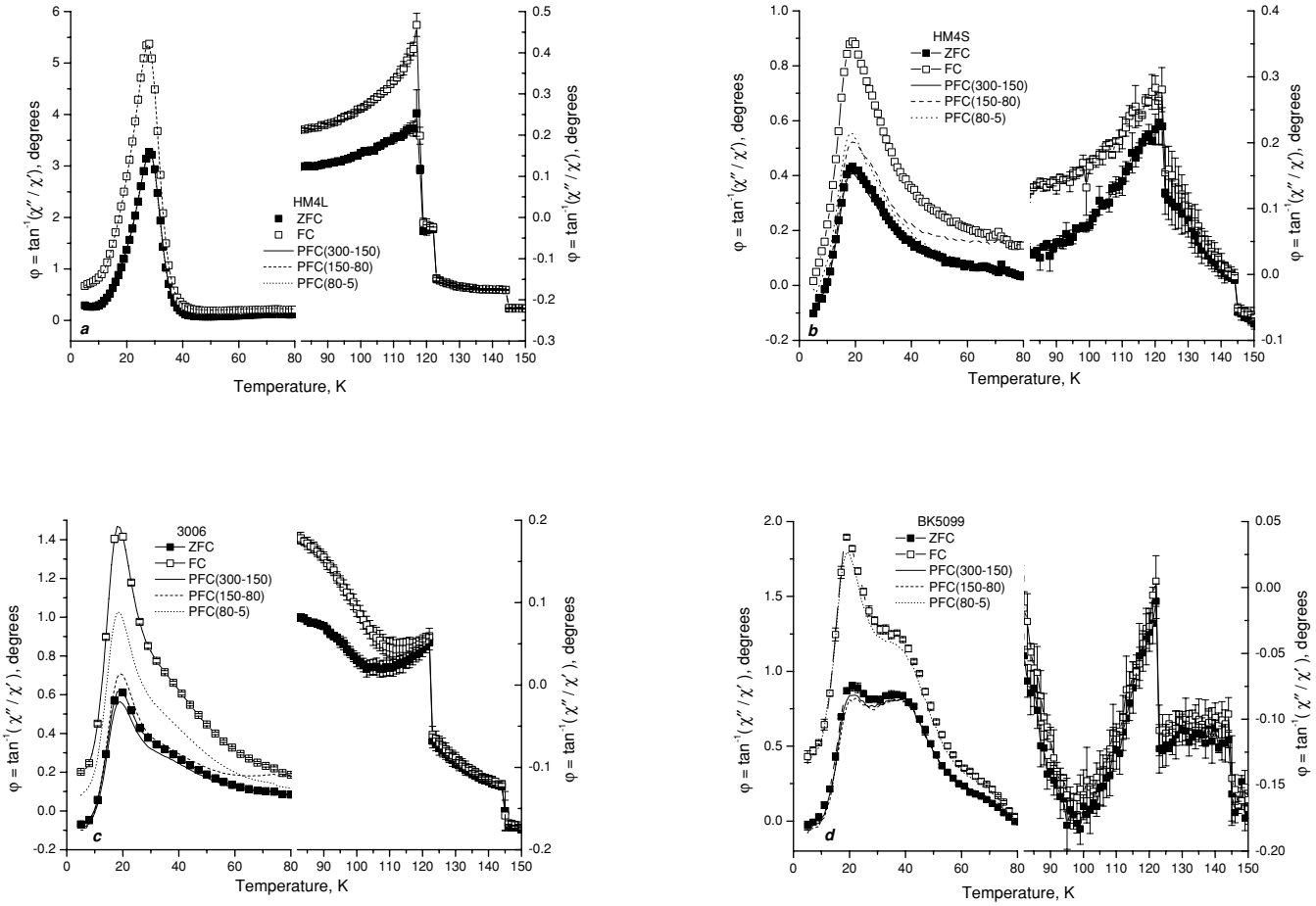


**Figure 6.** Temperature dependences of the out-of-phase susceptibility after different thermomagnetic treatments. Only ZFC and FC curves are shown above 80 K. Note also different vertical scales below and above 80 K.

ideal case (Walz & Kronmüller 1991; Walz 2002), two jumps observed in HM4L may simply be due to the two phases with slightly different stoichiometry.

### 5.2 Frequency dependences

The frequency dependence of the in-phase susceptibility is shown in Fig. 7. At room temperature, the susceptibility generally decreases with decreasing frequency. However, the decrease over five decades of frequency, from $10^3$ to $10^{-2}$ Hz, is 0.5–0.7 per cent at most for the PSD samples and about 2 per cent for the MD sample HM4L. This is very similar to the previous studies (Bhathal & Stacey 1969; Worm *et al.* 1993); however, in the present study much lower frequencies have been used. Close to the Verwey transition and at an intermediate temperature below it (75 K for BK5099 and 70 K for the three other samples) the susceptibility of the PSD samples increases slightly with the frequency decrease (by 1–4 per cent over the frequency range studied, not shown in the figure). For HM4L, the susceptibility at 70 K also increases with decreasing frequency by about 2 per cent. In contrast, at 117 K, i.e. just below the Verwey transition, the susceptibility first drops sharply, then decreases more gently and finally nearly flattens below *ca.* 10 Hz.

At the two lowest temperatures, all four samples show quite different behaviour, which in addition depends on the cooling mode. At 10 K, the frequency dependence is essentially flat down to 2 Hz, and then starts to increase almost linearly with log frequency. The rate of increase is largest for HM4L, where, in the case of FC, it amounts to about 4.5 per cent per frequency decade. For the PSD samples, the increase rate for the FC state is about half that for HM4L. Compared with FC, the increase rate for the ZFC state in the low-frequency range is 1.5–4 times smaller, depending on the sample. At 30 K the three PSD samples show a more or less steady increase with decreasing frequency over the whole range studied. Again, the increase for the ZFC state is about half that for FC. In the MD sample HM4L, however, susceptibility is saturated below *ca.* 1 Hz for both ZFC and FC, albeit at different levels normalized to the $10^3$ Hz value.

## 6 DISCUSSION

Thermal demagnetization of the saturation remanent magnetization acquired at a low temperature has become a fairly common method for characterizing the magnetic mineralogy of rock samples. However, in most cases only phase transitions are sought, while the overall temperature variation of SIRM is rarely analysed in detail. Generally, SIRM is acquired only after cooling in a zero magnetic field (ZFC), limiting the information which can be drawn from the low-temperature magnetization data.

Cooling in a strong magnetic field (FC) is known to affect many materials of interest to rock magnetism, such as magnetite (Li 1932), titanomagnetites (Schmidbauer & Readman 1982), goethite (Rochette & Fillion 1989) and siderite (Housen *et al.* 1996). In

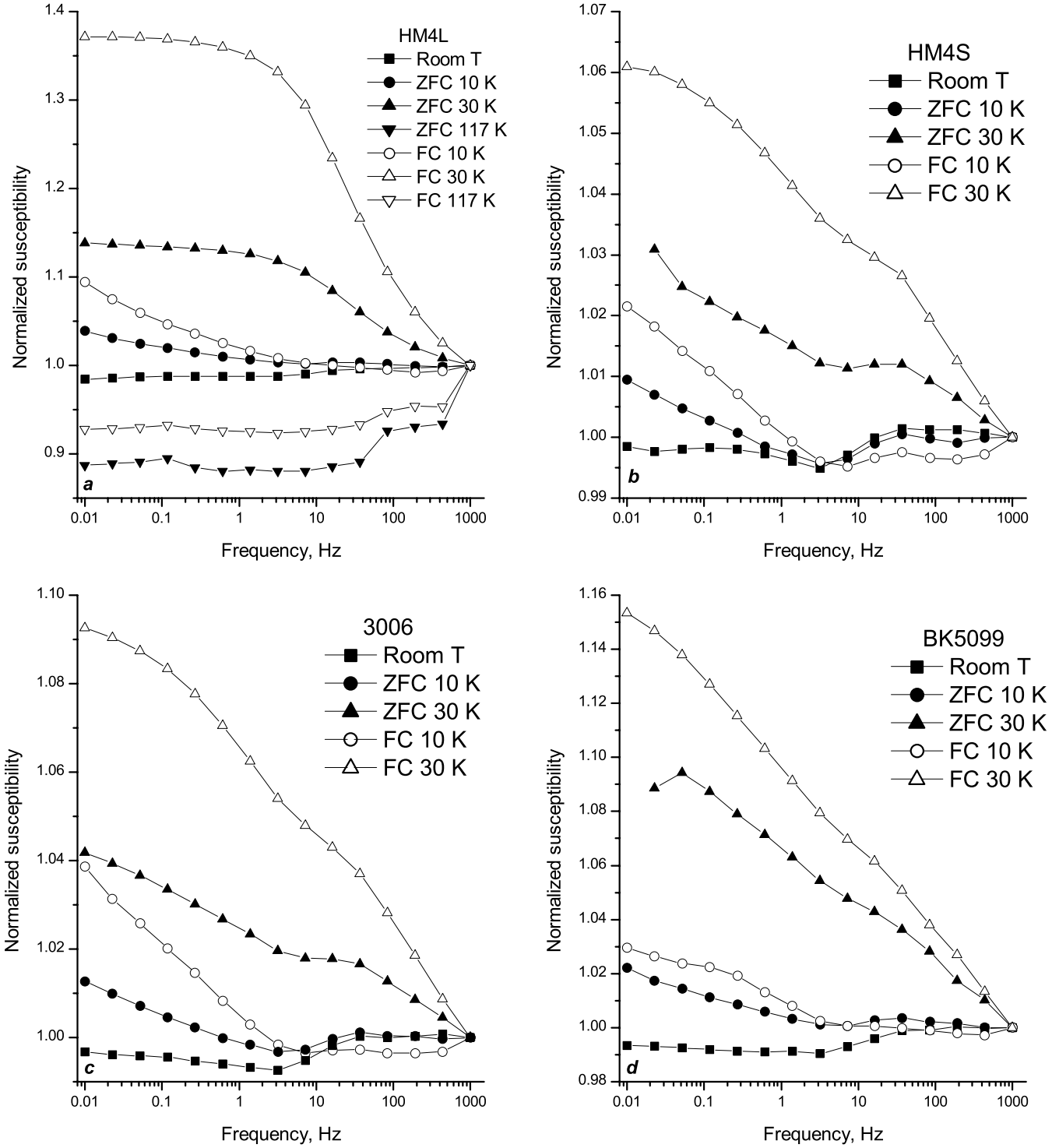


**Figure 7.** Frequency dependence of the in-phase susceptibility at selected temperatures.

the case of magnetite, demagnetization of SIRMs acquired after ZFC and FC, respectively, has been suggested as a test for its biogenic origin (Moskowitz *et al.* 1993). Characterizing the amount of magnetization lost at the Verwey transition by the parameter $\delta = \frac{\mathrm{SIRM(80\,K)-SIRM(150\,K)}}{\mathrm{SIRM(80\,K)}}$, biogenic magnetite has been found to show the ratio $\delta_{\mathrm{FC}}/\delta_{\mathrm{ZFC}} > 2$, while in single-domain and small pseudo-single-domain grains of inorganically produced magnetite this ratio ranges from 1 to 1.6 (Moskowitz *et al.* 1993; Carter-Stiglitz *et al.* 2002). If the low-temperature SIRM($T$) curves are to be used to constrain the unmixing of magnetic data on natural samples (Carter-Stiglitz *et al.* 2001), more data and a better understanding of the magnetic properties of the low-temperature phase of magnetite as related to grain size and stoichiometry are required.

SIRM demagnetization curves bear a fundamental difference from temperature dependences of hysteresis parameters, since the initial magnetic state of a sample is only modified by changes in

temperature. It is therefore instructive to compare SIRM($T$) behaviour observed in the present study with the hysteresis properties of the same four samples reported previously (Kosterov 2001, 2002).

In the multidomain sample HM4L, SIRM($T$) shows little variation below the Verwey transition, independent of the preceding thermomagnetic treatment. Similarly, the $M_{rs}/M_s$ ratio and the coercive force are nearly constant up to about 80 K, where easy magnetization axes set during the initial cooling through the transition apparently become switchable again (Kosterov 2001). SIRM(5 K) after FC is smaller than that after ZFC by a factor of 2, and nearly the same relationship holds for $M_{rs}/M_s$ ratios derived from the hysteresis loops measured as a function of temperature. During SIRM demagnetization, however, switching of easy axes does not occur since the whole experiment is performed in a zero magnetic field. This explains why a decrease of SIRM prior to the Verwey transition, as compared with the $M_{rs}/M_s$ ratio, is relatively less pronounced and occurs at somewhat higher temperatures.

Samples HM4S and 3006, despite a difference in their Verwey temperatures, show quite similar magnetic properties below the transition. Thus, a superficial maghemite layer present in 3006 (Smirnov & Tarduno 2002) apparently does not influence the behaviour of the magnetite core below the Verwey transition. Composition of the latter, assuming the Verwey temperature of 110 K, corresponds to a $\Delta$ value of about 0.003 in the formula $Fe_{3(1-\Delta)}O_4$ (Aragón *et al.* 1985; Aragón 1992). Note that this is a maximum estimate since stresses also lower $T_V$ (Samara 1968; Tamura 1990; Rosenberg *et al.* 1996). Magnetocrystalline anisotropy of the low-temperature phase of such a material is only 15 per cent lower than for the stoichiometric magnetite (Kąkol & Honig 1989). This difference is probably too small to be reliably sensed in hysteresis, SIRM or susceptibility measurements on isotropic assemblages of fine magnetite grains. Results for these two samples will therefore be treated together.

SIRM($T$) curves of the two samples measured after ZFC and FC, respectively, are very similar, SIRM (5 K) after FC being only about 5 per cent higher than that after ZFC. The difference between FC and ZFC curves disappears at about 70–80 K, well below the Verwey transition. SIRMs after PFC(150–80 K) nearly equal those after FC, being, however, much more thermally stable. SIRMs after PFC(80–5 K) are again very similar to those after FC, both in magnitude and in stability. This behaviour can be explained assuming that in magnetite grains several microns in size new easy magnetization axes can develop under the action of a strong magnetic field well below the Verwey transition. However, thermal stability of the easy axes is higher the closer to the transition they are formed.

Hysteresis measurements on the same samples with a Princeton Measurements VSM (Kosterov 2001, 2002) have shown that at 10 K SIRMs, derived from loops measured after FC, are significantly (by about 20 per cent) higher than after ZFC. The temperature variation of the $M_{rs}/M_s$ ratios in the two experiments is also different. $M_{rs}/M_s$ after FC decreases much more rapidly but converges with the ZFC curve only at the Verwey transition. To reconcile these observations with SIRM($T$) data, hysteresis loops for the sample 3006 were measured at 10 K after ZFC and FC treatments using an MPMS XL instrument. The $M_{rs}/M_s$ ratio was found to be 0.252 after FC, and 0.236 after ZFC. These values are approximately in the same proportion as SIRMs acquired by simply setting the magnetic field to zero, but are considerably smaller than the respective $M_{rs}/M_s$ ratios measured with a VSM (0.392 and 0.323, respectively). Such a large difference is likely to be due to a much faster field setting in the VSM instrument compared with an MPMS. Hysteresis measurements with a VSM thus sample a quasi-instantaneous distribution of easy magnetization axes and pinning sites, while in an MPMS measurement easy axes distribution apparently has time to accommodate to a changing field environment. This behaviour is, however, seen only in pseudo-single-domain and smaller grains.

The ratio of SIRMs acquired below the Verwey transition after FC and ZFC, respectively (FC/ZFC ratio, for short) can be evaluated theoretically only for the simplest case of Stoner–Wohlfarth (Stoner & Wohlfarth 1948) particles, which are essentially uniaxial particles for which the magnetic moment can only be reversed by the rotation-in-unison mechanism. Two assumptions have to be made: (1) after ZFC easy magnetization axes are directed at random, while after FC they follow the [001] directions of the high-temperature cubic phase closest to the magnetic field applied during cooling and (2) no easy axes can be switched into a new direction by SIRM acquisition field. Under these assumptions, the theoretical FC/ZFC ratio for an assemblage of SW particles should be 1.664. However, experimental values observed for the stoichiometric magnetite are much lower. Even for $53 \times 35 \times 35$ nm$^3$ biogenic magnetite grains (magnetotactic bacterium strain MV1) that had been expected to behave like ideal single-domain particles, Moskowitz *et al.* (1993) reported values of about 1.25. Recent measurements (Carter-Stiglitz *et al.* 2002) have yielded FC/ZFC ratios of 1.36 for magnetite from the same bacterial strain MV1 and 1.29 for the strain MS1. These samples may, however, be oxidized due to several years of storage, as suggested by their lowered Verwey temperatures of 105 and 97 K, respectively. Magnetostatic interactions in particle chains, typical for biogenic magnetite, might be suggested as a tentative reason for the lowering of FC/ZFC ratio in these samples. Two magnetite samples of inorganic origin containing mostly single-domain grains yielded FC/ZFC ratios of 1.42 and 1.47, respectively (Carter-Stiglitz *et al.* 2002). For larger, 250 nm magnetite grains the FC/ZFC ratio derived from hysteresis measurements (Schmidbauer & Keller 1996) is even higher, about 1.6. This may be in part due to the fact that these measurements were made with a VSM, rather than with an MPMS, although a 1 min pause had been taken after the field change. These grains are, however, too large to be single domain even below the Verwey transition, in agreement with a recent micromagnetic model (Muxworthy & Williams 1999). More experimental data are needed to elucidate the factors controlling the FC/ZFC ratio in single-domain magnetite.

FC/ZFC ratios of about unity, observed in the present study on pseudo-single-domain grains several microns in size, may be viewed as intermediate between the two extremes representing, respectively, very fine (single-domain) and very large (true multidomain) grains. Magnetostatic interactions in pseudo-single-domain and larger grains seem unlikely to affect the low-temperature magnetic properties in a significant way. The major contribution to an exterior magnetic field created by a multidomain ferromagnetic grain comes from and acts primarily upon the domains close to the grain boundaries. The SIRM value, on the other hand, is determined by interactions between adjacent domains within a given grain, which generally outweigh interactions between the grains. On the experimental side, King & Williams (2000) have found that in interacting 250 nm magnetite cubes at 50 nm spacing loss of SIRM at the Verwey transition is only a few per cent larger than in non-interacting grains of the same size. At the same time, in both cases normalized SIRM($T$) curves were essentially flat below approximately 100 K.

Properties of the low-temperature phase of sample BK5099 strongly differ from those of HM4S and 3006. Its most striking feature is a very large difference between ZFC and FC SIRM($T$) curves. The FC/ZFC ratio amounts to 1.74, i.e. even higher than the

theoretical limit for Stoner–Wohlfarth particles. The $\delta_{FC}/\delta_{ZFC}$ ratio is 1.75, somewhat higher than previously reported for magnetites of inorganic origin (Moskowitz *et al.* 1993; Carter-Stiglitz *et al.* 2002). SIRM acquired at 5 K after PFC(150–80 K) demagnetizes even more strongly on passing the Verwey transition, yielding the $\delta_{PFC}/\delta_{ZFC}$ ratio of 1.86. At the same time, hysteresis measurements below the Verwey transition (Kosterov 2002) yielded for this sample $M_{rs}/M_s$ ratios between 0.25 and 0.35, dependent on the thermomagnetic history, precluding the possibility of single-domain behaviour. Existing hysteresis (Schmidbauer & Schembera 1987; Özdemir *et al.* 2002) and SIRM($T$) (Özdemir *et al.* 2002) data for stoichiometric magnetite with a comparable or smaller grain size are also fairly different from those shown by BK5099. It may be suggested therefore that in this highly non-stoichiometric sample ($T_V = 95$ K, corresponding to $\Delta$ about 0.006 in the formula $Fe_{3(1-\Delta)}O_4$ (Aragón *et al.* 1985; Aragón 1992) the magnetic field applied during cooling exerts much stronger control over setting new easy magnetization axes in the low-temperature phase, so that easy axes can deviate from the [001] direction of the cubic phase towards the direction of magnetic field applied during cooling. Resulting tighter concentration of easy axes around the cooling field direction would explain the larger remanence. The behaviour of susceptibility measured after different treatments also supports this hypothesis. The difference between susceptibilities measured after FC and ZFC, respectively, is about 35 per cent, which is about twice as high as in more stoichiometric samples. At the same time, easy axes initially formed on passing the Verwey transition are far less stable than in stoichiometric magnetite, as indicated by FC and ZFC susceptibility curves almost converging at about 40 K, much lower than the Verwey temperature for this sample (95 K).

The physical mechanism of the peculiar behaviour of magnetization and susceptibility in this highly non-stoichiometric sample is most probably the magnetocrystalline anisotropy of the low-temperature phase, which shows a strong decrease with increasing non-stoichiometry (Kąkol & Honig 1989). In magnetite with a $\Delta$ of about 0.006 in formula $Fe_{3(1-\Delta)}O_4$, corresponding to the Verwey temperature of 95 K, the magnetocrystalline anisotropy constant $K_a$, the largest of the five monoclinic magnetocrystalline anisotropy constants, is only about 60 per cent that of the stoichiometric magnetite. Kąkol & Honig (1989) have also observed the onset of easy axes switching around 40 K. ZFC and FC susceptibility curves in BK5099 converge at about this temperature.

## 7 CONCLUSION

Saturation isothermal remanent magnetization and AC susceptibility curves have been measured as a function of temperature between 5 K and room temperature on four samples of multidomain and pseudo-single-domain magnetite. The emphasis has been made on the role of a magnetic field applied during cooling through the Verwey transition in forming the magnetic state of the magnetite low-temperature phase. In multidomain grains, the effect of cooling (complete or partial) in a strong magnetic field on SIRM and susceptibility data below the Verwey transition, as well as on the magnetic hysteresis properties measured previously (Kosterov 2001), can be adequately understood by assuming that on passing the Verwey temperature from above easy magnetization axes of the low-temperature phase are set along the [001] directions of the cubic phase closest to the direction of applied magnetic field (Bickford 1950; Williams *et al.* 1953). However, as PFC(80–5 K) SIRM and susceptibility versus temperature curves show, easy magnetization axes can also be set in new directions by applying a strong field well below the Verwey transition. Pseudo-single-domain grains display a more complex behaviour, as revealed by differences between FC, PFC(150–80 K) and PFC(80–5 K) SIRM and susceptibility versus temperature curves. In this case, easy magnetization axes formed by a magnetic field applied during cooling through the Verwey temperature can be easily reset by switching off the field at an intermediate temperature. Conversely, easy axes can be set into new directions by a partial field cooling starting at a temperature well below $T_V$. Both effects are greatly enhanced in oxidized magnetite due to the much lower magnetocrystalline anisotropy of its low-temperature phase.

## ACKNOWLEDGMENTS

This study was initiated during the author's stay at the Geological Survey of Japan, made possible through a Science and Technology Agency (Japan) postdoctoral fellowship. At Tokyo Institute of Technology AK has been supported by a Japan Society for the Promotion of Science (JSPS) postdoctoral fellowship. I am grateful to Toshitsugu Yamazaki, Hirokuni Oda and Hideo Tsunakawa for many scientific and technical discussions. Mark Dekkers (University of Utrecht) kindly made available samples of HM4 magnetite. Sample of 3006 magnetite was obtained from Alexei Smirnov and BK5099 from Masayuki Torii. I am grateful to Özden Özdemir for the information on the history of the BK5099 sample. I thank Brian Carter-Stiglitz for providing the raw magnetization data from Carter-Stiglitz *et al.* (2002). This paper has benefited from reviews by Adrian Muxworthy and an anonymous reviewer.

## REFERENCES

Abe, K., Miyamoto, Y. & Chikazumi, S., 1976. Magnetocrystalline anisotropy of low temperature phase of magnetite, *J. Phys. Soc. Jpn.,* **41,** 1894–1902.

Aragón, R., 1992. Magnetization and exchange in nonstoichiometric magnetite, *Phys. Rev. B,* **46,** 5328–5333.

Aragón, R., Buttrey, D.J., Shepherd, J.P. & Honig, J.M., 1985. Influence of nonstoichiometry on the Verwey transition, *Phys. Rev. B,* **31,** 430–436.

Bhathal, R.S. & Stacey, F.D., 1969. Frequency independence of low-field susceptibility of rocks, *J. geophys. Res.,* **74,** 2025–2027.

Bickford, L.R., Jr, 1950. Ferromagnetic resonance absorption in magnetite single crystals, *Phys. Rev.,* **78,** 449–457.

Calhoun, B.A., 1954. Magnetic and electric properties of magnetite at low temperatures, *Phys. Rev.,* **94,** 1577–1585.

Carter-Stiglitz, B., Moskowitz, B. & Jackson, M., 2001. Unmixing magnetic assemblages and the magnetic behavior of bimodal mixtures, *J. geophys. Res.,* **106,** 26 397–26 411.

Carter-Stiglitz, B., Jackson, M. & Moskowitz, B., 2002. Low-temperature remanence in stable single domain magnetite, *Geophys. Res. Lett.,* **29,** doi: 10.1029/2001GL014197.

Creer, K.M. & Like, C.B., 1967. A low temperature investigation of the natural remanent magnetization of several igneous rocks, *Geophys. J. R. astr. Soc.,* **12,** 301–312.

Cui, Y., Verosub, K.L. & Roberts, A.P., 1994. The effect of low-temperature oxidation on large multi-domain magnetite, *Geophys. Res. Lett.,* **21,** 757–760.

de Boer, C.B. & Dekkers, M.J., 1996. Grain-size dependence of the rock magnetic properties for a natural maghemite, *Geophys. Res. Lett.,* **23,** 2815–2818.

Domenicali, C.A., 1950. Magnetic and electrical properties of natural and synthetic single crystals of magnetite, *Phys. Rev.,* **78,** 458–467.

Dunlop, D.J., 1995. Magnetism in rocks, *J. geophys. Res.,* **100,** 2161–2174.

Dunlop, D.J., 2002. Theory and application of the Day plot ($M_{rs}/M_s$ versus

$H_{cr}/H_c$) 1. Theoretical curves and tests using titanomagnetite data, *J. geophys. Res.,* **107,** doi: 10.1029/2001JB000486.

Halgedahl, S.L. & Jarrard, R.D., 1995. Low-temperature behavior of single-domain through multidomain magnetite, *Earth planet. Sci. Lett.,* **130,** 127–139.

Hartstra, R.L., 1982. Grain-size dependence of initial susceptibility and saturation magnetization-related parameters of four natural magnetites in the PSD–MD range, *Geophys. J. R. astr. Soc.,* **71,** 477–495.

Heider, F., Dunlop, D.J. & Soffel, H.C., 1992. Low-temperature and alternating field demagnetization of saturation remanence and thermoremanence in magnetite grains (0.037 mkm to 5 mm), *J. geophys. Res.,* **97,** 9371–9381.

Housen, B., Banerjee, S.K. & Moskowitz, B.M., 1996. Low-temperature magnetic properties of siderite and magnetite in marine sediments, *Geophys. Res. Lett.,* **23,** 2843–2846.

Kąkol, Z. & Honig, J.M., 1989. Influence of deviation from ideal stoichiometry on the anisotropy parameters of magnetite $Fe_{3(1-\delta)}O_4$, *Phys. Rev. B,* **40,** 9090–9097.

King, J.G. & Williams, W., 2000. Low-temperature magnetic properties of magnetite, *J. geophys. Res.,* **105,** 16 427–16 436.

Kobayashi, K. & Fuller, M., 1968. Stable remanence and memory of multidomain materials with special reference to magnetite, *Philos. Mag.,* **18,** 601–624.

Kosterov, A.A., 2001. Magnetic hysteresis of pseudo-single-domain and multidomain magnetite below the Verwey transition, *Earth planet. Sci. Lett.,* **186,** 245–253.

Kosterov, A.A., 2002. Low-temperature magnetic hysteresis properties of partially oxidized magnetite, *Geophys. J. Int.,* **149,** 796–804.

Li, C.H., 1932. Magnetic properties of magnetite crystals at low temperature, *Phys. Rev.,* **40,** 1002–1012.

Mauritsch, H.J. & Turner, P., 1975. The identification of magnetite in limestones using the low-temperature transition, *Earth planet. Sci. Lett.,* **24,** 414–418.

Moloni, K., Moskowitz, B.M. & Dahlberg, E.D., 1996. Domain structures in single crystal magnetite below the Verwey transition as observed with a low-temperature magnetic force microscope, *Geophys. Res. Lett.,* **23,** 2851–2854.

Morrish, A.H. & Watt, L.A.K., 1958. Coercive force of iron oxide micropowders at low temperatures, *J. Appl. Phys.,* **29,** 1029–1033.

Moskowitz, B.M., Frankel, R.B. & Bazylinski, D.A., 1993. Rock magnetic critetia for the detection of biogenic magnetite, *Earth planet. Sci. Lett.,* **120,** 283–300.

Moskowitz, B.M., Jackson, M. & Kissel, C., 1998. Low-temperature magnetic behavior of titanomagnetites, *Earth planet. Sci. Lett.,* **157,** 141–149.

Muxworthy, A.R., 1999. Low-temperature susceptibility and hysteresis of magnetite, *Earth planet. Sci. Lett.,* **169,** 51–58.

Muxworthy, A.R. & McClelland, E., 2000. The causes of low-temperature demagnetization of remanence in multidomain magnetite, *Geophys. J. Int.,* **140,** 115–131.

Muxworthy, A.R. & Williams, W., 1999. Micromagnetic models of pseudo-single-domain grains of magnetite near the Verwey transition, *J. geophys. Res.,* **104,** 29 203–29 217.

Nagata, T., Kobayashi, K. & Fuller, M.D., 1964. Identification of magnetite and hematite in rocks by magnetic observations at low temperature, *J. geophys. Res.,* **69,** 2111–2120.

Özdemir, Ö. & Banerjee, S.K., 1982. A preliminary magnetic study of soil samples from west-central Minnesota, *Earth planet. Sci. Lett.,* **59,** 393–403.

Özdemir, Ö. & Dunlop, D.J., 1998. Single-domain-like behavior in a 3-mm natural single crystal of magnetite, *J. geophys. Res.,* **103,** 2549–2562.

Özdemir, Ö. & Dunlop, D.J., 1999. Low-temperature properties of a single crystal of magnetite oriented along principal magnetic axes, *Earth planet. Sci. Lett.,* **165,** 229–239.

Özdemir, Ö., Dunlop, D.J. & Moskowitz, B.M., 1993. The effect of oxidation on the Verwey transition in magnetite, *Geophys. Res. Lett.,* **20,** 1671–1674.

Özdemir, Ö., Dunlop, D.J. & Moskowitz, B.M., 2002. Changes in remanence, coercivity and domain state at low temperature in magnetite, *Earth planet. Sci. Lett.,* **194,** 343–358.

Ozima, M. & Ozima, M., 1965. Origin of thermoremanent magnetization, *J. geophys. Res.,* **70,** 1363–1369.

Ozima, M., Ozima, M. & Akimoto, S., 1964a. Low-temperature characteristics of remanent magnetization of magnetite—self-reversal and recovery phenomena of remanent magnetization, *J. Geomag. Geoelectr.,* **16,** 165–177.

Ozima, M., Ozima, M. & Nagata, T., 1964b. Low temperature treatment as an effective means of 'magnetic cleaning' of natural remanent magnetization, *J. Geomag. Geoelectr.,* **16,** 37–40.

Radhakrishnamurty, C., Likhite, S.D., Deutsch, E.R. & Murthy, G.S., 1981. A comparison of the magnetic properties of synthetic titanomagnetites and basalts, *Phys. Earth planet. Inter.,* **26,** 37–46.

Rochette, P. & Fillion, G., 1989. Field and temperature behavior of remanence in synthetic goethite: Paleomagnetic implications, *Geophys. Res. Lett.,* **16,** 851–854.

Rosenberg, G.K., Hearne, G.R., Pasternak, M.P., Metcalf, P.A. & Honig, J.M., 1996. Nature of the Verwey transition in magnetite ($Fe_3O_4$) to pressures of 16 GPa, *Phys. Rev. B,* **53,** 6482–6487.

Sahu, S., 1997. An experimental study of the effects of stress on the magnetic properties of magnetite, *PhD thesis,* University of Minnesota.

Samara, G.A., 1968. Effect of pressure on the metal–nonmetal transition and conductivity of $Fe_3O_4$, *Phys. Rev. Lett.,* **21,** 795–797.

Schmidbauer, E. & Keller, R., 1996. Magnetic properties and rotational hysteresis of $Fe_3O_4$ and $\gamma$-$Fe_2O_3$particles ~250 nm in diameter, *J. Magn. Magn. Mater.,* **152,** 99–108.

Schmidbauer, E. & Readman, P.W., 1982. Low temperature magnetic properties of Ti-rich Fe-Ti spinels, *J. Magn. Magn. Mater.,* **27,** 114–118.

Schmidbauer, E. & Schembera, N., 1987. Magnetic hysteresis properties and anhysteretic remanent magnetization of spherical $Fe_3O_4$ particles in the grain size range 60–160 nm, *Phys. Earth planet. Inter.,* **46,** 77–83.

Senanayake, W.E. & McElhinny, M.W., 1981. Hysteresis and susceptibility characteristics of magnetite and titanomagnetites: interpretation of results from basaltic rocks, *Phys. Earth planet. Inter.,* **26,** 47–55.

Senanayake, W.E. & McElhinny, M.W., 1982. The effects of heating on low-temperature hysteresis and susceptibility properties of basalts, *Phys. Earth planet. Inter.,* **30,** 317–321.

Šimša, Z., Zounová, F. & Krupička, S., 1985. Initial permeability of single-crystal magnetite and Mn-ferrite, *Czech. J. Phys. B,* **35,** 1271–1281.

Skumryev, V., Blythe, H.J., Cullen, J. & Coey, J.M.D., 1999. AC susceptibility of a magnetite crystal, *J. Magn. Magn. Mater.,* **196–197,** 515–517.

Smirnov, A.V. & Tarduno, J.A., 2000. Low-temperature magnetic properties of pelagic sediments (Ocean Drilling Programme Site 805C): tracers of maghemitization and magnetic mineral reduction, *J. geophys. Res.,* **105,** 16 457–16 471.

Smirnov, A.V. & Tarduno, J.A., 2002. Magnetic field control of the low-temperature magnetic properties of stoichiometric and cation-deficient magnetite, *Earth planet. Sci. Lett.,* **194,** 359–368.

Stoner, E.C. & Wohlfarth, E.P., 1948. A mechanism of magnetic hysteresis in heterogeneous alloys, *Phil. Trans. R. Soc. Lond.,* A, **240,** 599–642.

Tamura, S., 1990. Pressure dependence of the Verwey temperature of $Fe_{3-y}O_4$ obtained by magnetic permeability measurements, *J. Phys. Soc. Jpn.,* **59,** 4462–4465.

Verwey, E.J.W., 1939. Electronic conduction of magnetite ($Fe_3O_4$) and its transition point at low temperatures, *Nature,* **44,** 327–328.

Walz, F., 2002. The Verwey transition—a topical review, *J. Phys.: Condens. Matter,* **14,** R285–R340.

Walz, F. & Kronmüller, H., 1991. Evidence for a single-stage Verwey-transition in perfect magnetite, *Philos. Mag. B,* **64,** 623–628.

Weiss, P. & Forrer, R., 1929. La saturation absolue des ferromagnétiques et les lois d'approche en fonction du champ et de la température, *Ann. Phys.*, 10, **12,** 279–374.

Williams, H.J., Bozorth, R.M. & Goertz, M., 1953. Mechanism of transition in magnetite at low temperatures, *Phys. Rev.,* **91,** 1107–1115.

Worm, H.-U., Clark, D. & Dekkers, M.J., 1993. Magnetic susceptibility of pyrrhotite: grain size, field, and frequency dependence, *Geophys. J. Int.,* **114,** 127–137.